Chapter 13
Radiation Shielding and Protection, Part I: Measurement, Dosimetry, Shielding, and Protection

Christopher J. Watchman

Contents

13.1 Fundamental Radiation Protection Principles 371
13.2 Medical Radiation Sources 372
13.3 Dose 373
13.4 Radiation Dosimetry 374
13.5 Radiation Detection 384
13.6 Radiation Shielding 393
Additional Reading 402

Shielding and protection are essential to the safe practice of radiation oncology, radiology, and other medical specialties that use radiation. Medical health physics is essentially the study and practice of radiation safety as it relates to the use of radiation in medicine. This encompasses two distinct areas: (1) physical methods of measuring and calculating radiation dose and (2) the regulatory environment. In this chapter the physics methods will be discussed. Areas discussed will include (1) radiation measurement and its associated devices; (2) radiation dosimetry, both external and internal; and (3) radiation shielding design.

13.1 Fundamental Radiation Protection Principles

13.1.1 Time

Exposure to radiation as a function of time increases the number of interaction that occurs. Consequently, there is an increased amount of damage that may result. Reduction of time of exposure is the simplest method to reduce radiation dose to an individual or area. This can be accomplished by different methods including simply

C.J. Watchman, PhD, DABR (✉)
Department of Radiation Oncology, University of Arizona, Tucson, AZ, USA
e-mail: watchman@email.arizona.edu

M. Maqbool (ed.), *An Introduction to Medical Physics*, Biological and Medical Physics, Biomedical Engineering, DOI 10.1007/978-3-319-61540-0_13

limiting time in a radiation field to physical controls that limit access to the radiation field. Minimizing exposure time is also the most cost-effective method of radiation safety.

13.1.2 Distance

Maximizing distance between the radiation source and the individual or object is the next basic radiation safety principle. Radiation fields decrease from a sources as a function of $1/r^2$. Therefore increasing distance by a factor of two decreases the radiation exposure by a factor of one fourth. Maximizing distance may be done by process controls, physical barriers, or other methods.

13.1.3 Shielding

Shielding involves placing a physical barrier between the radiation source and the area/personnel/public that needs to be protected. The goal is to reduce the overall exposure of radiation to the subject. Shielding can be quite expensive depending on the source of radiation. For photon applications high-Z materials are needed to reduce the intensity of the photon. Beta particles on the other hand may only require thin sheets of plastic. Energy of the particles also plays an important role. For example 100 KeV photons may only require a thin sheet of lead to reduce their intensity to acceptable levels. High-energy photons from a linear accelerator used in radiation therapy may require meters of concrete to do the same job. Radiation shielding is a major undertaking and will be discussed in greater depth at the end of this chapter.

13.2 Medical Radiation Sources

In medicine sources of radiation are varied in their origin, physical type, application, and dangers. Different areas of medicine where radiation is normally used include radiology, radiation oncology, nuclear medicine, cardiology, and interventional radiology. These examples are by no means the only disciplines that may use radiation but are the most common specialties that do. In radiology the sources of radiation are primarily artificially produced by machines. These sources tend to be of an energy range on the order of 20–200 kVp. Interventional radiology is also included in this but may also involve the use of radioactive isotopes as well. Nuclear medicine primarily uses unsealed sources of radioactivity. Unsealed describes the state of the radioactive isotope being “uncontained” but is freely combined with a pharmaceutical compound. Energies seen in this discipline are on

Table 13.1 Common medical isotopes

Isotope	Energy	Particle	T1/2	Application
^{131}I	364 keV (82%) / 192 keV(89%)	γ/β	*8.02 day*	Hyperthyroidism, Grave's disease
^{125}I	35 keV/150.61 keV	γ/β	*59.4 day*	Radioimmunoassay, brachytherapy
^{99m}Tc	140 keV	γ	*6.01 h*	Multiple medical imaging applications
^{192}Ir	380 keV (avg)	γ	*73.83 day*	High-dose rate brachytherapy
^{32}P	1.709 MeV	β	*14.29 day*	Nuclear medicine, biochemistry
^{18}F	633.5 keV/511 keV	$\beta+/\gamma$	*1.83 h*	Positron emission tomography imaging

the order of ~500 keV. Cardiology applications are actually nuclear medicine applications used for heart problem diagnosis. Radiation oncology, the practice of treating cancer with radiation, is somewhat different than the other specialties discussed in that it uses both sealed and unsealed isotopes and it uses a much broader range of energies than in the others (~50 keV to 20 MeV). In Table 13.1 is a list of common radiation isotopes used in medicine.

Depending on the form/type of radiation, a different hazard is present. The basic hazard types may be broken down into internal hazard or external hazard types. Internal hazard radiation is of little risk when it is present outside of the body, but when it is internalized, it can deliver a significant dose of radiation. An example of this would be an alpha particle emitting radionuclide. Despite having high energy, alpha particles travel only small distances due to their large charge. Consequently, a sheet of paper is capable of blocking them. Lighter charged particles are also internal hazards but do travel farther than alpha particles. Photons on the other hand are usually considered external hazards to do their exponential absorption rate through matter. Neutrons are also external hazards and behave similarly to photons. In medicine each of these hazard types may be present. As a result it is imperative that proper methods be used to measure, calculate dose, and create protective measures for each.

13.3 Dose

Radiation dose in its fundamental form can be described by the following equation:

$$D = \lim_{m \to 0} \frac{dE}{dm} \tag{13.1}$$

Where E is energy deposited (units J or MeV or eV), m is mass (units g, kg), and D is dose (units J/kg or Gy or MeV/g). Note that in Eq. A, the value of dose is a point value in space. Consequently, it is more of a theoretical definition that should

more accurately be described by the value average dose since the energy deposition over the volume may not be uniformly distributed. Equation 13.1 could more usefully be written as

$$\langle D \rangle = \frac{dE}{dm} \text{ or } \bar{D} \frac{\int_{E_0}^{E} dE}{\int_{0}^{m} dm} \tag{13.2}$$

Or more simply as

$$\langle D \rangle = \frac{E}{m} \tag{13.3}$$

Thus, average absorbed dose will simply be referred to as dose from this point on.

Calculation of dose is dependent on the particle type being evaluated. Dose calculations for photons, electrons, neutrons, and heavy charged particles each rely on different physical phenomena and therefore are calculated differently. Each will be discussed below, but before this we must define the basic descriptors for radiation fields.

13.4 Radiation Dosimetry

Radiation dosimetry is the process whereby radiation energy deposited in matter is either measured or calculated. In this section computational methods for determining radiation dose will be presented. In medical health physics applications, how radiation dose is calculated can be separated into two categories: (1) external methods where the radiation source is outside the body and (2) internal methods where the radiation source is inside the body.

13.4.1 External Radiation Dosimetry

13.4.1.1 Radiation Field Descriptors

A radiation field may be described in terms of particles or energy radiance. Particle or N is simply the number of particles in the field. Radiance or R is the number of particles multiplied by their energy. For example, 10^6 particles of 1 MeV per particle would result in a radiance of 10^6 MeV.

$$\Phi = \frac{dN}{da} \quad \left(\frac{\#}{\text{cm}^2}\right) \tag{13.4}$$

Another way to describe a radiation field is by how many particles pass a unit area. This is called fluence. Fluence and its units are given in Eq. 13.4.

Time can also be used to describe the field in terms of the number of particles passing by the unit area. This is called flux and it has units of particles per second.

$$\dot{N} = \frac{dN}{dt} \quad \left(\frac{\#}{s}\right) \tag{13.5}$$

Each of these also has their correlate in terms of radiance termed the energy flux and energy fluence as shown in the two equations below:

$$\dot{R} = \frac{dR}{dt} \quad (\text{watts}) \tag{13.6}$$

and

$$\Psi = \frac{dR}{da} \quad \left(\frac{\text{MeV}}{\text{cm}^2}\right) \tag{13.7}$$

Lastly, and generally most usefully, we can describe the field in terms of time and area. This is called the flux density or fluence rate as shown in the following equation:

$$\phi = \frac{d}{dt}\left(\frac{dN}{da}\right) \quad \left(\frac{\#}{\text{cm}^2 - \text{s}}\right) \tag{13.8}$$

The radiance equivalent is called the energy fluence rate as shown below:

$$\Psi = \frac{d}{dt}\left(\frac{dR}{da}\right) \quad \left(\frac{\text{MeV}}{\text{cm}^2 - \text{s}}\right) \tag{13.9}$$

The use of these radiation field descriptors allows us to calculate dose from each of the radiation particles we will discuss starting with photons.

13.4.1.2 Photons

Photons interact with matter by way of exponential attenuation which is the reduction in number of photons passing through a material. The attenuation rate is dependent on the attenuation coefficient μ $(1/x)$ where x is the depth in a material. Equation 13.10 describes the process, and Fig. 13.1 presents an example of the decrease in number of photons with depth for three different μ.

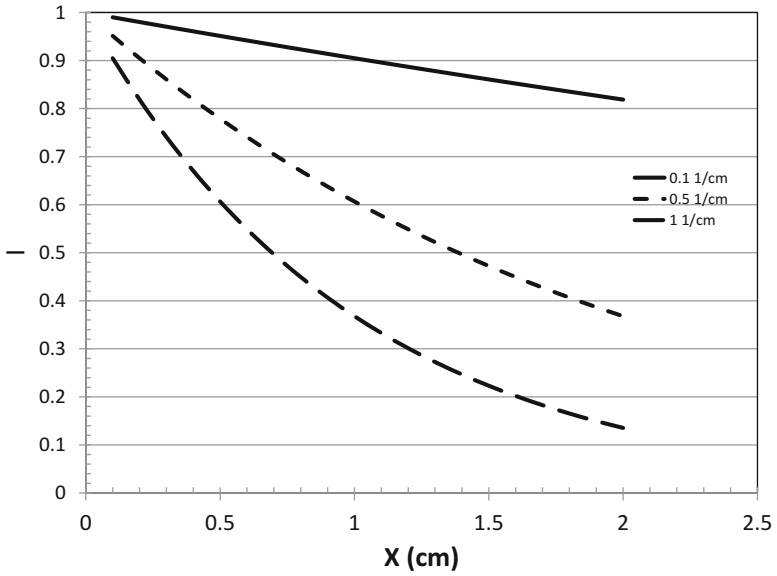

Fig. 13.1 Exponential attenuation for $\mu = 0.1\ \text{cm}^{-1}$, $0.5\ \text{cm}^{-1}$, and $1\ \text{cm}^{-1}$

$$I = I_0 e^{-\mu x} \tag{13.10}$$

The attenuation coefficient is the sum of the interaction probabilities of each of the types of photon interactions that can occur and represents the rate at which photons leave the primary field. Therefore,

$$\mu = \sigma + \tau + \kappa + \sigma_R$$

or the combination of Compton scatter, photoelectric effect, pair production, and Rayleigh scattering. Each of these interaction processes may or may not transfer energy to the material that it interacts with. Consequently we need to track the energy that is transferred to the system, and this is called the attenuation transfer coefficient as shown in Eq. 13.11.

$$\mu_{\text{tr}} = \tau_{\text{tr}} + \kappa_{\text{tr}} + \sigma_{\text{tr}} \tag{13.11}$$

Note that the Rayleigh scattering component is no longer part of the equation since this interaction does not transfer energy.

Although energy is transferred to the system or material the photon field is encountering, that energy may not remain in the system but escape. Only energy that remains in the system will result in energy deposition or in other words dose to the material. Photon energy may escape by simply continuing to pass through the material. Scattered photons may also escape the system, or bremsstrahlung may occur. Bremsstrahlung occurs when electrons encounter a coulombic field and

change direction, and in order to conserve momentum and energy, a photon is released. These photons may then escape the system. Due to this escape fraction on the energy transferred to the material system, another attenuation factor has been described to show the energy that remains in the system, and it is called the energy absorption coefficient as shown it the equation below:

$$\mu_{\text{en}} = \mu_{\text{tr}}(1 - g) \tag{13.12}$$

Here the value g represents the average secondary electron energy lost to bremsstrahlung and other radiative processes, one last item to note in regard to the attenuation coefficients. Most often they are written in terms of per mass or in other words the mass attenuation (μ/ρ), mass transfer (μ_{tr}/ρ), and mass energy absorption coefficients (μ_{en}/ρ). This is done to eliminate the mass dependence of these coefficients for both ease of use in dose calculations and so that coefficients for different materials may be more easily compared. From this point on, these will all be referred to by their mass coefficient name.Using these different parameters we can begin to calculate radiation dose from photons for different radiation fields. Equation 13.13 shows the basic calculation for photon dose based upon the mass energy absorption coefficient, energy, and fluence:

$$D = \frac{d\varepsilon}{dm} = \Psi\frac{\mu_{\text{en}}}{\rho} = \Phi E\frac{\mu_{\text{en}}}{\rho} \tag{13.13}$$

Note that e is the energy imparted to the system and that the energy fluence can be broken down into the fluence and particle energy. If the field contained multiple energies, you would need to integrate over the energy regime. This would require a new μ_{en} for each of the energies used. We can use unit analysis to determine the final units of dose based on the above equation where:

$$\frac{\gamma}{\text{cm}^2} \bullet \frac{\text{J}}{\gamma} \bullet \frac{\text{cm}^2}{\text{kg}} = \frac{\text{J}}{\text{kg}} = \text{Gy}$$

The gray is the standard unit of dose for radiation measurement and is consistent with the SI unit system.

We can also look at dose in terms of the rate at which the field is interacting with a material. The equation is the same as Eq. 13.13 except that we use fluence rate/flux density in the place of fluence. Equation 13.14 shows this:

$$\dot{D} = \frac{d\varepsilon}{dmdt} = \psi\frac{\mu_{\text{en}}}{\rho} = \phi E\frac{\mu_{\text{en}}}{\rho} \tag{13.14}$$

And we can similarly analyze the units.

$$\frac{\text{J}}{\text{cm}^2\text{s}} \bullet \frac{\text{cm}^2}{\text{kg} \bullet \text{s}} = \frac{\text{J}}{\text{kg} \bullet \text{s}} = \frac{\text{Gy}}{\text{s}}$$

Alternate methods for photon dose calculation are all dependent on these basic principles and can be derived based on the above methods.

Reference values for mass attenuation coefficients are available from the National Institute of Standards and Technology (NIST) in their XCOM database located online at http://www.nist.gov/pml/data/xcom/index.cfm.

13.4.1.3 Electrons

When discussing electron dose we must realize that we are talking about particles that may either collide inelastically or elastically. Inelastic collision results when some of the particles kinetic energy is lost in the interaction. This may be by way of ionization, excitation, or conversion to photons (bremsstrahlung). Elastic collisions on the other hand do not lose energy but are capable of redistributing energy among the particles in the collision. This is classically looked at as the billiard ball example.

Unlike photons, which are neutral, electrons have a negative charge associated with them. Consequently, their primary mode of interaction is with the Coulomb field of the atom or nucleus or other electrons depending on how far the electron passes with respect to the atomic nucleus. In cases where the electron passes very far from the nucleus, we get what are termed "soft collisions." These interactions occur with respect to the outermost electrons of the atom, and the energy transferred to them is locally absorbed. Each one of these collisions is small resulting in a very small amount of energy transferred per collision. Despite the small energy transfer, these collisions are high probability and result in high numbers of collisions. If the electron passes closer to the atom in the area of the inner orbital electron shells, we begin to get harder collisions known as "Hard Collisions or knock on collisions." These types of collisions result in substantial energy loss but are lower probability and fewer in number as compared to soft collisions. Notwithstanding, these collisions can result in some of the energy being lost by way of delta rays, characteristic x-rays, and auger electrons.

If the electron passes even closer, on the order of the atomic radius, we begin to see direct interaction with the coulombic field of the nucleus. In this collision scenario, the majority of collisions are elastic (~97%) proportionally to Z^2. Here both energy and momentum are conserved with slight energy loss. In the other 3% of cases, we have bremsstrahlung occur. Note that these percentages are approximate and are dependent on the material.

Unlike photon dose, electron dose requires the use of a different parameter than attenuation. This is due to the small deflection paths caused by soft collisions. In order to calculate electron dose, we must define stopping power or mass stopping power. Equation 13.15 shows mass stopping power which is the spatial rate of energy loss:

$$\frac{S}{\rho} = \frac{dT}{\rho dx} \tag{13.15}$$

Where S/ρ is mass stopping power, T is the electron kinetic energy, ρ is the density of the material, and x is the distance in the material. In this equation we must note that dT and dx are finite energies and distances, respectively. The mass stopping power consists of two components: collisional and radiative. Collisional losses are the interactions discussed earlier excluding the radiative losses described by bremsstrahlung and the other radiative process. It is important to note that mass collisional stopping power for electrons is greater for low-Z materials than for high-Z materials. Radiative mass stopping power is the opposite and is proportional to EZ^2.

The simplest use of stopping power to calculate electron dose is found in Eq. 13.16:

$$D = \frac{\Phi\left(\frac{dT}{\rho dx}\right)_c}{\rho t}\rho t = \Phi\left(\frac{dT}{\rho dx}\right)_c \tag{13.16}$$

where t is a small thickness of the medium the electrons are entering and c signifies the collisional components of mass stopping power and the other parameters that have previously been described. Here the units of the solution are in MeV/g, but a conversion factor or 1.602×10^{-10} can be applied to change the units to Gy. For mathematical simplicity, this conversion factor will not be used in the following descriptions. Equation 13.16 gives us the dose for a thin layer of medium, but as we add layers, the solution becomes more of an average dose as individual electrons travel very different paths in their particle tracks leaving different amounts of energy at depth. So if these small layers are put together into thicker layers, we get the following average dose relationship:

$$\bar{D} = \Phi_c \frac{\Delta T_c}{\rho t} = \Phi \frac{T_0(1 - Y(T_0))}{\rho t} \tag{13.17}$$

where T_0 is the initial energy and $Y(T_0)$ is the radiative yield. As the thickness of the material becomes ever greater, we then can integrate over these other thicknesses to achieve the dose at some depth x as shown in Eq. 13.18.

$$D_x = \Phi\left(\frac{dT}{\rho dx}\right)_{c,m} \tag{13.18}$$

Here x is the depth and m is the medium.

Reference values for electron mass stopping powers and other electron dosimetry values are available from NIST in their ESTAR database located online at http://physics.nist.gov/PhysRefData/Star/Text/ESTAR.html.

13.4.1.4 Heavy Charged Particles

Dose calculations for charged particles that are heavier than the electron (HCP) also rely on stopping power. Unlike electrons an approximation is used to calculate dose in a medium. This is called the continuous slowing down approximation (CSDA), and it shown in Eq. 13.19.

$$R_{\mathrm{CSDA}} = \int_0^{T_0} \left(\frac{dT}{\rho dx}\right)^{-1} dT \tag{13.19}$$

The CSDA assumes that uniform energy deposition and linear particle tracks occur. For HCPs this is a reasonable assumption due both to their heavy mass and charge. Using this approximation we can then calculate and average dose through a thin medium as

$$\bar{D} = \Phi \frac{\Delta T \cos\theta}{\rho t} \tag{13.20}$$

where ΔT is the difference between the range through the medium and the remaining energy of the particle as it passes through the thin medium. If the particle does not enter perpendicularly, then the addition of the $\cos\theta$ is needed.

This description of dose is acceptable for thin mediums, and as the medium increases we see a change in the behavior of the energy deposition. At the end of the particles energy, it begins to deposit large amount of its energy and peaks near the end of its path. This is called the Bragg peak, and a full discussion of the dose calculation for this is beyond the scope of this chapter and will not be discussed further.

Reference values for protons and alpha particle mass stopping powers and other dosimetry values are available from NIST in their PSTAR and ASTART database located online at http://physics.nist.gov/PhysRefData/Star/Text/PSTAR.html and http://physics.nist.gov/PhysRefData/Star/Text/ASTAR.html, respectively.

13.4.1.5 Neutrons

Neutrons are neutral nucleons that can be produced by different interaction in medical health physics, specifically by high-energy photons and protons. These interactions result in varying energy regimes that make simple dose calculations very difficult and beyond the scope of this chapter. Generally these calculations require Monte Carlo or discrete linear Boltzmann methods. Therefore in medical health physics, measurement of these fields and doses is the methodology of choice and will be discussed in the radiation detection and measurement section.

13.4.2 Internal Radiation Dosimetry

Internal radiation dose is more complicated than external dose due to the inclusion of not only the physics but also the biology of the subject. Consequently, we can break down internal radiation dose into two components. First, a component that includes the biology of the subject and the total number of nuclear transitions. The second is a physical dose conversion factor that gives the total energy deposited per unit mass for a specific source and target combination. Two systems were developed to do these dose calculations, but both are simply the same physics with different descriptions. These two methods are the International Commission on Radiological Protection (ICRP) method and the Medical Internal Radiation Dose (MIRD) method. Equations 13.21 and 13.22 show both of these methods.

$$H_T = U_s \text{SEE} \tag{13.21}$$

$$D = \tilde{\text{A}}\text{S}(r_t \leftarrow r_s) \tag{13.22}$$

Each of these equations breaks down into two components, one that relates the total number of nuclear transformations and the other that relates the energy deposition within the material. In Eqs. 13.21 and 13.22, the first portion is represented by U_s and $\tilde{A}$ that are called the number of decays and the accumulated activity, respectively. The energy deposition portions are SEE – specific effective energy – and S ($r_t \leftarrow r_s$) the S-value. Each of these values further breaks down into an absorbed fraction and the mass of the target tissue/organ. This is shown below:

$$S = EY\frac{\phi(r_t \leftarrow r_s)}{m_t} = \Delta_i \frac{\phi(r_t \leftarrow r_s)}{m_t} \tag{13.23}$$

Where E is the energy of the radiation particle, Y is the yield of the particle, m_t is the mass of the target, and $\phi(r_t \leftarrow r_s)$ is the fraction of the initial energy E that is absorbed in the target. Δ_i is the product of EY. If multiple energies are part of the radiation isotope or isotopes being calculated, the above equation would need to be integrated over each energy and yield along with their corresponding absorbed fraction. In Fig. 13.2 is a simple illustration of the interplay between a source and target.

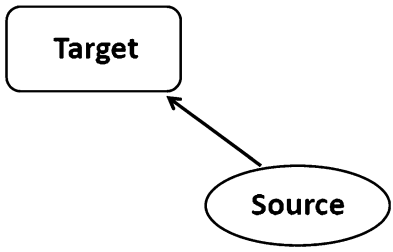

Fig. 13.2 Simple interplay between source and target

Note that in the above figure, the radiation particles may pass between the source to the target and deposit energy. Loss of energy between the source/target combination results in an absorbed fraction that is less than 1. The absorbed fraction may be 1 if and only if there is self-absorption of the radiation in the target. This methodology may be used for photon, beta emitters, and alpha emitters.

When comparing these two methodologies, the physics remains the same, but the objective in the dose calculation is different. In the MIRD system the end point of the calculation is to evaluate some biological end point of the dose. For example, dose from an isotope may result in suppression of the bone marrow. On the other hand, the ICRP methodology is looking at estimates of radiation risk to a person or population. Consequently, the ICRP method has greater uncertainty in what the dose means since the time and amount of radiation received can be variable or unknown, unlike the MIRD objective where the radiation quantity is known. Despite these differences for the purposes of this chapter, we will use the MIRD mathematics to describe internal dose.

Internal dosimetry innately means that the radiation dose has been incorporated into the body. How the radiation entered the body can vary from ingestion, injection, inhalation, absorption, and through wounds. Each of these pathways allows for the radioactive material to enter the body and then enter the blood stream. Translocation of the radiation through the blood allows for dispersion of the radiation throughout the entire body. Preferential deposition of the radiation in different areas and organs of the body is dependent on the nature of the radioactive material, chemical composition, and physical properties. Chemical composition alters how the body and the radioactive material interact and can allow for quicker or slower deposition, retention, and loss of the material in an organ or body region. The physical properties, such as Z, can also directly change where the isotope deposits. For example, materials that are in the column of the periodic table such as Ca would also preferentially deposit in regions of high Ca content such as the bones. ^{90}Sr and ^{226}Ra would be examples of such isotopes. The physical decay of the isotope along with the biological half-life also plays a role in the dose. The physical half-life is an innate property of the isotope, while the biological half-life describes how the isotope leaves the body or organ, and it is reliant on the previously discussed parameters.

How the radiation enters the body and then is translocated is the biological part of the internal dose calculation. To obtain this information, we have different biological modeling methods. First we can directly measure radiation from the body and apply modeling (curve fits) to obtain the accumulated activities in each organ and in the whole body. The second methodology is to use biokinetic or pharmacokinetic models with known model and transfer parameters. Fortunately there are several published compartmental models describing the major pathways for intake of radioactive materials into the body. The International Commission on Radiological Protection (ICRP) has models for the following intake pathways: respiration, wounds, and ingestion. They also provide biokinetic models for many different elements and some organ specific models. One can obtain these reports on their website at http://www.icrp.org/publications.asp.

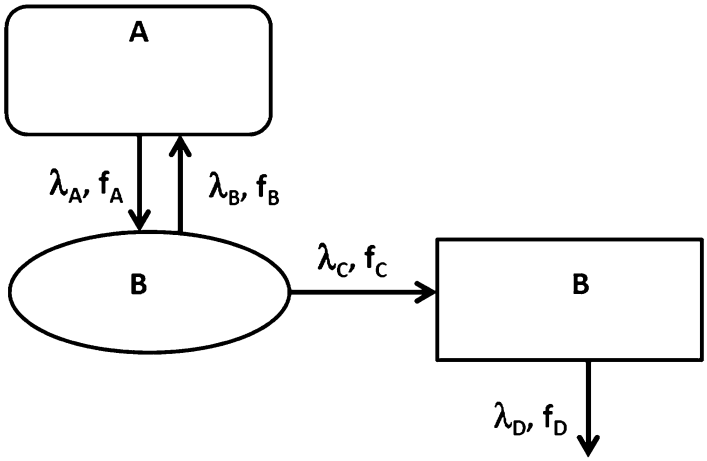

Fig. 13.3 Simple three-compartment internal dosimetry kinetics model

Models of this nature may be complex or fairly simplistic. We will discuss a simple three-compartment model as an example. Figure 13.3 illustrates the model.

In this figure three different compartments are present. Each compartment can contain radioactive material. The arrows indicate paths of translocation between the compartments and out of the system. Each of these paths has a transfer constant (λ) (similar to a decay constant) and a retention function (f) which describes the fraction of the material that remains in the compartment. Each of these functions is time dependent, so this needs to be accounted for. Note that there is also a possibility of material going back and forth between two different compartments, and this must be included in any solution. Material may also exit the system completely as shown in the arrow exiting compartment three. This is often an excretion pathway.

A series of kinetic equations may be developed to describe the behavior of this system as shown below in this series of equations:

$$\frac{dA}{dt} = -f_A A\lambda_A \tag{13.24}$$

$$\frac{dB_A}{dt} = f_B B\lambda_B \tag{13.25}$$

$$\frac{dB}{dt} = f_A A\lambda_A - f_B B\lambda_B - f_C C\lambda_C \tag{13.26}$$

$$\frac{dC}{dt} = f_B B\lambda_B - f_C C\lambda_C - f_D C\lambda_D \tag{13.27}$$

In these equations λ is a combined decay constant that includes both physical decay and physiological half-life, ABC are the compartment activity content, and f is the fraction of the activity uptake in the compartment of the total activity that entered the body.

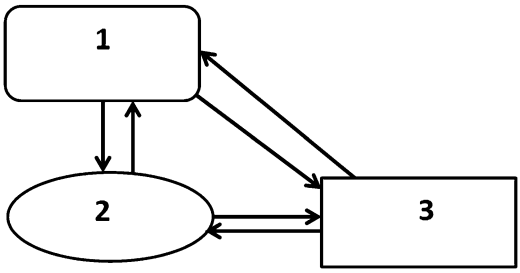

Fig. 13.4 Multiple target irradiation from different source compartments

Once the kinetics component of the calculation is determined, then the physics of the energy deposition may be addressed. Figure 13.4 shows that each compartment may irradiate the other resulting in multiple components to the dose of the target.

Here we see that compartment 1 may irradiate compartments 2 and 3 as well as itself. The same holds true for each of the other compartments. As a result, each of the absorbed fractions from the source compartment must be individually calculated and then summed together to calculate the total dose from Eqs. 13.22 and 13.23.

13.5 Radiation Detection

As discussed in a previous chapter, ionizing radiation interacts with matter by way of several mechanisms depending on the particle type. Detection of radiation relies upon these interaction types, and each measurement tool is specifically designed to take advantage of these interactions. In this section we will focus on the basic detectors used in medical health physics.

13.5.1 Gas-Filled Chambers

One of the most commonly used methods for detecting radiation is to use a gas-filled chamber and a voltage potential difference across the chamber to measure current changes in the presence of radiation. Separation of positive and negative ions which are then moved through the electric field potential allows for the measurement of current. The amount of current and the relationship to the potential allow for different types of gas-filled detectors. Two different detectors are most commonly used, an ionization chamber and a Geiger-Muller tube. Other detectors can be used but will not be discussed here as they are infrequently used in medical health physics.

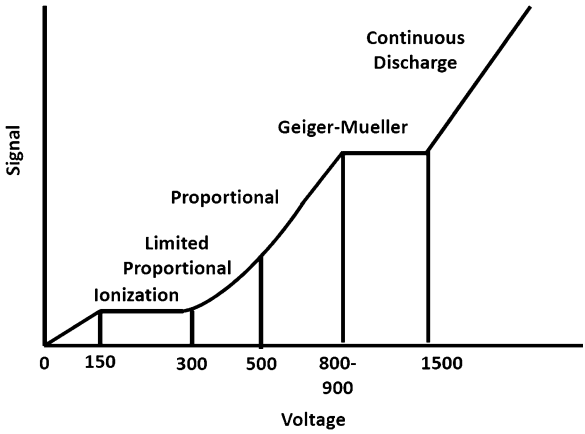

Fig. 13.5 Ionization curve for detection

Gas-filled chambers rely upon the breaking down of the gas by the incoming radiation particle into ion pairs. Then an applied electric field separates the ions as they move toward the anode and cathode of the system. A resulting current is then obtained and can be measured to evaluate the radiation field. Depending on the operating voltage, as will be discussed next, the gas-filled chamber may be calibrated to several different parameters such as exposure (measure of ionization in air for photon energies <3 MeV), dose, or simply radiation counts.

In Fig. 13.5 seen below shows the relationship of operating voltage and measured signal for the full range of gas-filled chambers. Note that the ionization chamber runs at a much lower potential than the Geiger-Muller tube. In each region of the curve, the amount of ionization of the gas varies and results in significantly different behaviors. Consequently, each region has its specific useful application, and we will only discuss the most pertinent application to medical health physics.

13.5.2 Ionization Chambers

Ionization chambers are one of the most common devices used in medical health physics. They are gas-filled chambers that are sensitive and allow for absolute calibration of the ionization charge collected to dose. They operate in the low-voltage region of the curve shown in Fig. 13.5. Figure 13.6a illustrates the basic electrical diagram of an ion chamber. The basic design is simple, an enclosed chamber that may be sealed or open to the atmosphere, an anode, cathode, voltage potential, and some device to measure the current or charge developed. When radiation particles pass into the chamber region, they may ionize the gas. The amount of energy needed at a minimum to ionize the gas is called the W value or average energy lost per ion pair formed. It is sometimes listed W/e. The exact value of this is dependent on the gas used in the chamber. Most often air is the gas, and the

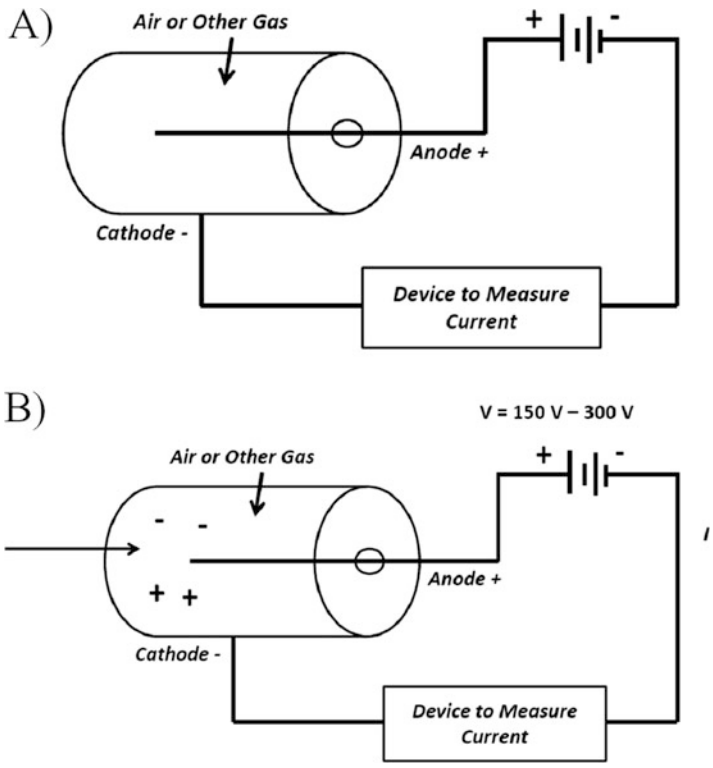

Fig. 13.6 (**a**) Schematic for basic ion chamber, (**b**) ionization and current in an ion chamber

required energy is 33.8 eV/ion pair. These ion pairs may recombine and not contribute the measured current. If the voltage is sufficient, then they are measured as part of the current. The operating voltage of 150–300 V is used for ion chambers and results in an accurate indication of the rate of ionization pairs created in the gas volume of the chamber. Figure 13.6b shows this relationship.

Ion chambers are most often used to for calibration of radiation-producing machines, to evaluate dose, and for evaluating radiation field exposures. Figure 13.7 shows two different types of ion chambers commonly used in medical health physics.

13.5.3 Geiger-Muller Detector

The Geiger-Muller (GM) detector, commonly referred to as the Geiger counter, is widely used as a radiation detection device. Unlike the ionization chamber, the GM detector does not allow for absolute calibration to dose. It is valued as a radiation detection device as it is highly sensitive to radiation and allows for easy detection of

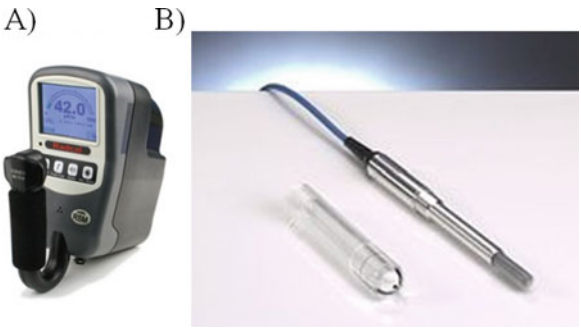

Fig. 13.7 (**a**) A survey ion chamber, (**b**) a farmer ionization chamber

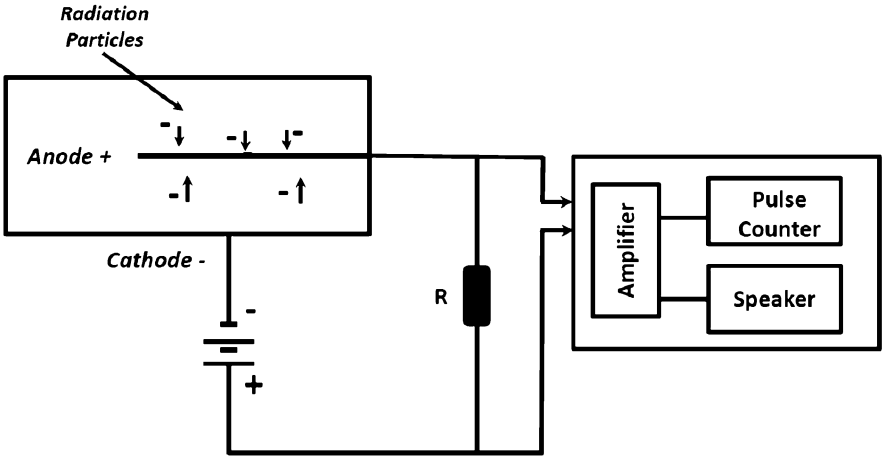

Fig. 13.8 GM detector schematic and discharge

the presence of radiation. Using a GM detector to locate small radiation fields has the analogy of using a flashlight in in a very dark room where the flashlight provides substantial contrast to the dark room. The GM detector does the same with respect to radiation; in other words, it readily identifies the region of radiation. Consequently, GM detectors are radiation locators or identifiers but do not give quantitative information about the amount of radiation or dose of radiation. These detectors have two methods of display for describing the intensity of the radiation field, a pulse counter or an audible speaker. The pulse counters usually have a range from 1 to100,000 counts. The audible alert is also useful as it increases in volume intensity with the increase in the counts of radiation and serves as a very efficient warning system.

As shown in Fig. 13.8, GM detectors also depend on the production of ion pairs in the gas-filled chamber, but due to the high-voltage potential used (Fig. 13.5: 800–1500 V), a single ion pair creates a large number of additional ion pairs. This process is called the Townsend avalanche, where a single ion pair causes a cascade

reaction of additional ion pairs that are then collected. These avalanches mean that GM detectors are highly sensitive to radiation as discussed earlier. One issue with this is that the gas can become fully ionized and any new radiation particles will not cause additional events to count. Consequently, two methods for quenching the gas and allowing for better detection are used. The first is to use an external RC circuit to decrease the potential across the resistor and allow for recombination of the gas. The alternate method is to include a quench gas into the chamber. This gas may be a polyatomic gas, organic gas, or halogen. These quench gases reduce the amount of photoelectrons produced in the avalanche thus reducing the total ionization of the chamber gas.

13.5.4 Semiconductor Detectors

Also widely used in medical health physics are semiconductor detectors which are solid-state devices. These detectors rely upon similar principles to gas-filled chambers except that they instead use "defects" in the crystal structure of the gas as the charge carrier. These "defects" are called holes, and electrons act as the other carrier. Figure 13.9 illustrates these devices. In Fig. 13.9a the basic design of the semiconductor detector is shown where there are two regions, the valence band and conduction band, separated by a small energy gap of ~1 eV. The valence band is the highest energy region where electrons can exist in the semiconductor, and the conduction band is the region where electrons do not exist in their normal energy state. The addition of energy into the semiconductor (Fig. 13.9b) greater than the energy gap will allow for electrons to move into the conduction band. A hole is then left in the valence band, and the resulting difference in the charge movement will result in an electrical signal that may be measured and calibrated to the amount of radiation encountered by the semiconductor detector.

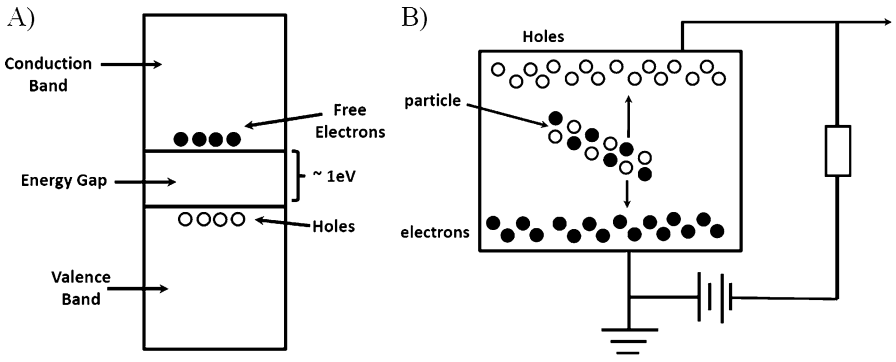

Fig. 13.9 (**a**) Simple illustration of the basic design of a semiconductor detector. (**b**) Illustration of the movement of holes and electrons in a semiconductor detector

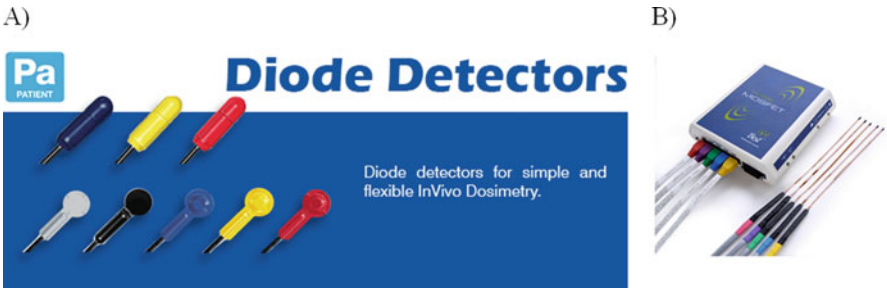

Fig. 13.10 (**a**) Diode detector from Sun Nuclear Corporation, (**b**) MOSFET detector from Best Medical LLC

Semiconductor detectors come in two different types, P-type and N-type. P-type semiconductors have a structure where there is an empty space in the structure (hole) that wants an electron to fill it in order to stabilize the structure. N-type semiconductor detectors, on the other hand, have an extra electron in the structure and want to lose that electron to the valence shell. In order for the semiconductor to work as a radiation detector, an electric field is applied which allows for the semiconductor to transport the electrons to the holes. This essentially makes the system a P-type semiconductor on one side of the device and an N-type on the other as seen in Fig. 13.9b. This is called the p-n junction.

Semiconductor detectors are widely used as they have small variations in signal response and good energy resolution. They also have the ability to resolve interactions quickly making their measurement time dependence very good. Common examples of these types of detectors are diode detectors or metal oxide field effect transistor (MOSFET) detectors as shown in Fig. 13.10 below.

13.5.5 Thermoluminescent Dosimeters

Another crystal structure radiation dose detector widely used in medical health physics is the thermoluminescent crystal dosimeter or TLD. TLDs are crystals that similar to semiconductor detectors have a valence and conduction band. Unlike semiconductor, TLDs have a series of intermediated energy traps within their crystal structure that allow for trapping of electrons in an excited state in the crystal. Figure 13.11a shows the basic arrangement of these crystals. These traps are impurities in the crystal structure that may hold onto electrons freed by incoming ionizing radiation or an electron/hole pair may be created as shown in Fig. 13.11b. Trapped electrons in this system allow for information about the amount of energy deposited into the crystal to be stored. This information may be released by heating the crystal which then emits light proportional to the dose received. To release the light a TLD reader, as shown in Fig. 13.12, is required.

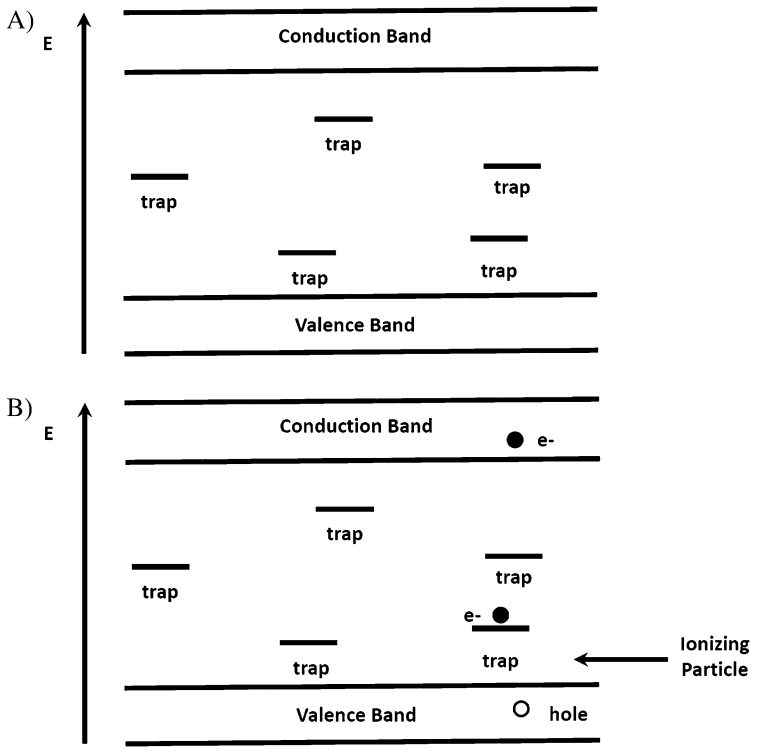

Fig. 13.11 (**a**) TLD crystal structure, (**b**) electron/hole traps with incoming radiation

The TLD reader consists of an oven for heating the crystals to release the trapped electrons. A thermocouple is used to measure the rate of heating of the crystals. Filters bring the emitted light into the effective measurement range of the photomultiplier tube (PMT). A high-voltage power supply to the PMT and a readout device are the remaining major components.

Readout of the emitted light is done by slowly heating the crystals to release the traps at a known rate. A glow curve is then generated that is a direct measure of the radiation dose to the crystals. Figure 13.13 shows a typical glow curve. Note that in the glow curve, there are different peaks which relate to different energy levels of the different traps in the crystal. The example in Fig. 13.13 is a fairly simple example with only two peaks, but more complicated glow curves are possible.

Optimal TLD crystals for dosimetry applications have a large linear range over a large dose range. They retain the trapped carriers during the temperatures of the irradiation. Additionally, they should produce large amounts of light and be able to be completely annealed following the reading of the crystal. Annealing is the final process where the crystal is returned to its baseline state by heating it to the point that all traps are released. This allows for the crystals to be reused regularly.

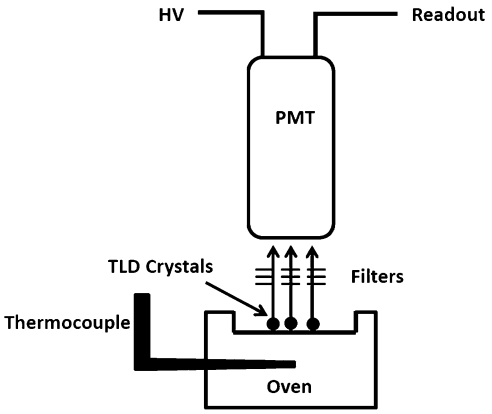

Fig. 13.12 TLD reader

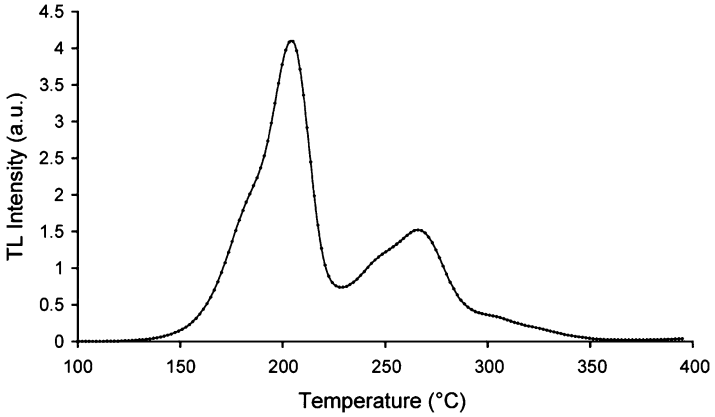

Fig. 13.13 TLD glow curve

Different types of crystals can be configured to specifically measure different types of radiation. Depending on the doping of the crystal, they could measure photon, beta particles, alpha particles, or neutrons. Typical TLD crystals include LiF, $Li_2B_4O_7$:Mn, Al_2O_3:C, CaF_2:Mn, CaF_2, $CaSO_4$:Mn, and $CaSO_4$:Dy. TLDs are most commonly used for area monitoring or personnel dosimetry.

13.5.6 Neutron Detectors

Neutrons, being neutral particles, can be very difficult to detect. Their interactions are based on ballistic interaction or absorption interactions. Two types of methods are commonly used to detect neutrons; these include proportional counters with gases sensitive to neutrons and activation foils. Activation foils, such as gold, rely

on the absorption of a neutron to activate the foil into an excited state where it will then become radioactive. Measurement of the radiation produced by the activated foil allows for measurement of the neutron field strength. This method is not commonly used in medical health physics and will not be discussed further. It should also be noted that semiconductor detectors can also be manufactured for neutron detection as well but are less common in medical health physics applications.

The more common tool used to measure neutrons is a proportional counter. In Fig. 13.5 the proportional range was after the ionization voltage range and was between 500 and 800 V. Over this range the potential is sufficient that additional ion pairs are created in a process called gas multiplication. Unlike the GM detector discussed earlier, the multiplication does not result in a Townsend avalanche but a proportional multiplication to the neutron field. This proportionality allows for calibration of the measured output to the neutron field strength.

The design of these proportional counters is similar to the ionization chamber in Fig. 13.6. Different gases than air are used due to their affinity for neutron absorption interactions. These most commonly include ^{3}He and ^{10}B. Equation 13.28 shows each of these interactions.

$$\begin{aligned} &^{3}\mathrm{He} + n = {}^{3}H + {}^{1}H + 0.764\mathrm{MeV} \\ &^{10}B + n = {}^{7}Li + \alpha \end{aligned} \tag{13.28}$$

Figure 13.14 shows that the boron also has an alternative excited state

One of the other common tools used to measure neutrons is the REM ball, which is so called as it is used to measure dose equivalent. It is also a proportional counter but is designed such that the readings relate units of rem instead of absorbed dose. REM is a unit of dose equivalent which estimates the biological effects of ionizing radiation. Figure 13.15 shows a cartoon of one.

In medical health physics, neutrons are generally only encountered when using high-energy linear accelerators in radiation oncology. Consequently, neutron

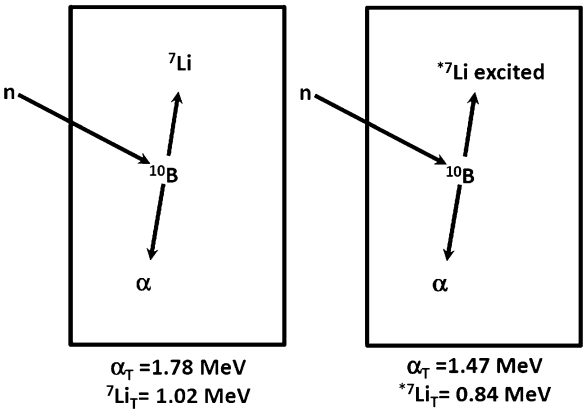

Fig. 13.14 Excited and baseline boron capture interaction used in neutron detection

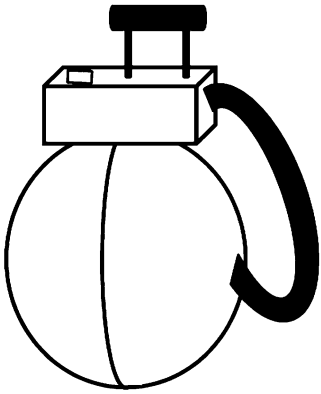

Fig. 13.15 REM ball

detectors are not common tools used by the medical health physicist except during machine commissioning or facility construction. Often these types of tools will need to be borrowed or rented.

13.6 Radiation Shielding

Radiation shielding is the process by which the intensity of radiation is reduced by the use of different materials. This consists of two parts: (1) shielding calculations and (2) shielding construction. Each will be discussed starting with shielding calculation methods.

13.6.1 Shielding Calculation Methods

Radiation shielding is specific to the type of radiation and energy of the particles. It can be further complicated by the presence of a mixed field of radiation types. Additionally, the type of facility also plays a large role in how these facilities are shielded. In medical health physics, we can define these facility types into the following categories: (1) diagnostic, (2) nuclear medicine, (3) radiation oncology, and (4) others. Guidance on how to do radiation shielding has been provided by the National Council on Radiation Protection (NCRP) in two documents. For diagnostic shielding NCRP Report 147 Structural Shielding Design for Medical X-ray Imaging Facilities is the core document used. When therapeutic of higher-energy photons are to be shielded NCRP Report 151 Structural Shielding Design and Evaluation for Megavoltage X- and Gamma-Ray Radiotherapy Facilities is the gold standard. Neither of these reports addresses positron emission tomography (PET), but in 2006 the American Association of Physicists in Medicine (AAPM) produced a Task Group Report entitled, "AAPM Task Group 108: PET and

PET/CT Shielding Requirements." This report is now the current standard reference for this type of shielding. This report is freely available at http://www.aapm.org/pubs/reports/RPT_108.pdf and will not be discussed in this chapter. The reader is strongly encouraged to review it. While these three reports tend to cover most situations that the medical health physicist will encounter, there are situations that fall outside of these reports. The specific principles and techniques discussed in the reports mentioned may be applied but interpreted to the situation. Prior to discussing each of these report methods, we will first discuss the common areas between these reports.

When planning any shielding project, the scope of the project must be clearly laid out. Shielding a diagnostic x-ray radiograph room is grossly different than that of a linear accelerator room. Even shielding a CT scanner room has differences, compared to a radiograph room, that need to be addressed to properly achieve ones goal. In the planning process, every attempt should be made to include the fundamental principles of time and distance in the design of the facility. Doing so will help to reduce the costs of the shielding component of the project. Assessment of budget, materials, location of rooms, types of radiation-producing devices, architecture design, and building construction issues will be needed. Key to this process is the understanding of the regulator limits, as discussed in an other chapter of this book, so that your design meets but does not exceed requirements. Exceeding requirements may result in a substantial increase in costs of the project.

For the purpose of shielding design, we break down areas that need to be protected into controlled and uncontrolled areas. A controlled area is a space where access is restricted to occupational exposures by radiation worker personnel. Uncontrolled areas are any other areas where the public may be, for example, hallways, exam rooms, and reception areas. Due to the open access, these areas require a stronger dose limit than controlled areas. In controlled areas for diagnostic imaging applications, the design goal (P) is 0.1 mGy air kerma strength per week. In therapeutic applications in controlled areas, P is 0.1 mSv per week or an annual 5 mSv per year. Note that the diagnostic application uses units of mGy and not the effective dose (mSv). This is due to the lower-energy regime of diagnostic beams as compared to therapy beams. Regardless, the 5 mSv per year recommendation is the same for both applications. Uncontrolled areas P are 0.02 mGy per week and 0.02 mSv per week for diagnostic and therapy, respectively. This design goal ensures that an annual limit of 1 mSv is not exceeded.

Upon completion of the project, a radiation survey is needed to ensure that the design goal was achieved. Failure of this survey may result in not obtaining a license or additional reconstruction costs to fix the problem. Consequently, these types of calculations should be done by a professional health, medical health, or medical physicist with experience in shielding calculations and design. It is recommended that all calculations be double-checked by additional parties in order to assist the shielding designer. Once the final survey is done and a license is issued, passive area monitoring of the room is warranted. This may be done with TLDs or other devices.

Certain commonalities are seen in both reports with respect to defined factors used in the calculations. One of these is the idea of occupancy factor (T) which is the fraction of beam on time that an area is occupied by an individual. It is used to better estimate the exposure to individuals. For fully occupied areas, such as offices, labs, x-ray control rooms, etc., a factor of 1 is given. This factor decreases with different areas. Patient exam rooms and treatment rooms have a T of 0.5, while corridors, patient rooms, employee lounges, and staff restrooms have a value of 0.2. Corridors are assigned a value of 0.125. Public restrooms, vending areas, storage rooms, outdoor seating, unattended waiting rooms, and patient holding rooms are given a T of 0.05. Other outdoor areas, unattended parking lots, janitor's closets, attics, unattended elevators, and stairways are assigned a value of 0.025.

We will now discuss each of these reports mentioned. Due to the extensive nature of each report, these discussions will only cover a basic introduction to the report. The reader is encouraged to probe deeper by obtaining these reports which will be listed at the end of this chapter.

13.6.1.1 NCRP 147 Methods

In NCRP 147 methodology, they identify specific position of interest outside of the shielded area where calculations should be made. This position is based upon the assumptions that the closest a person will nominally have their sensitive organs relative to the beam is <0.3 m from a wall, ≤ 1.7 m from the floor, and 0.5 m above the floor. It is considered unlikely or rare for any other combination of distances.

Shown in Fig. 13.16 is a typical configuration of a radiographic room with an x-ray source tube pointed toward the patient. Note that the patient is on top of a rectangular box in the picture. This represents the image receptor. Several

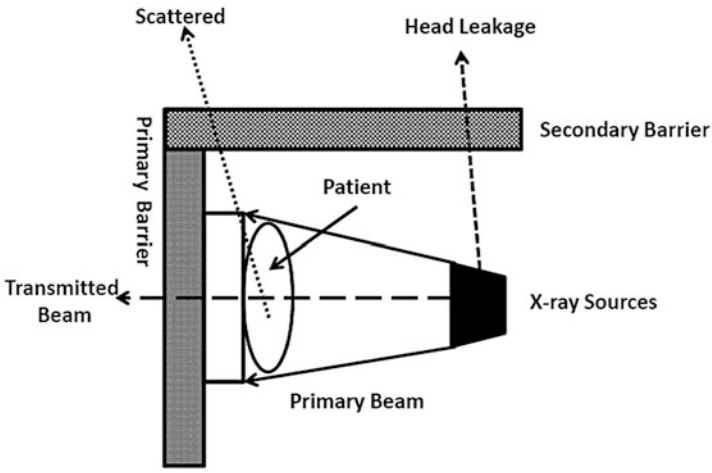

Fig. 13.16 Example radiographic room

important concepts to NCRP 147 are illustrated here. First is the transmittance through the patient from the primary beam. As is shown part of the primary beam passes through the patient, image receptor, and the barrier behind the image receptor. Transmitted primary beam passing through the wall is the reason for the addition of shielding materials to the wall. We define here the primary barrier as any wall or subregion of a wall where the primary beam is directed. A secondary barrier is any wall or region where scattered radiation may hit. Two types of scatter radiation exist, leakage and patient/object scatter. Leakage radiation comes from the x-ray tube itself due to scatter within it. Patient/object scatter comes from the primary beam hitting the patient/object, and partial scattering radiation interactions cause out scatter toward other barriers. It is important to account for all of this in the design goal shielding calculation.

Another important concept is the idea of workload (W) which is a factor that relates the x-ray tube's usage. Mathematically it is the time integral of the tube current with units of mA-min/week. To obtain W a survey of the department may be done, or standard values from NRCP 147 may be used. These standard values are radiographic rooms 277 mA-min/week, chest rooms 45 mA-min/week, and cardiac angiographic rooms 3050 mA-min/week. Equation NCRP 1 shows how to calculate this where W_{tot} is the total workload, N is the number of patients per week, and W_{norm} is the nominal workload for the system.

$$W_{\text{tot}} = NW_{\text{norm}} \tag{13.29}$$

NCRP 147 contains more detailed reference information for this concept.

The next factor that must be accounted for is the use factor (U) which relates the fraction of time the primary beam workload is directed to the primary barriers. Due to the primary beam hitting this region, it will require greater shielding to reduce the beam to the design goal. The report lists some typical U for the following barriers: chest image receptor 1.00, floor 0.89, and cross-table wall 0.09.

Figure 13.17 presents a typical radiographic room configuration and distances needed for the dose calculation.

In the figure we see multiple secondary barriers and an occupied control room. The control room is where the x-ray technician operates the system. Although not noted on in the diagram, the entire wall surrounding the control room is also secondary barriers. Several distances are shown in the diagram that relate to how the calculation is done. They are:

- d_{f} – distance from x-ray source to image receptor.
- d_{p} – distance from x-ray source to shielded area.
- d_{s} – patient scatter distance: this may be to any secondary barrier.
- d_{L} – leakage distance from x-ray source: this may be to any secondary barrier.
- F – the primary x-ray beam area.

These parameters will be used to get barrier thickness, but first we will go through how the thickness is calculated from basic physics. For the purposes of the transmitted beam through a barrier of some thickness, we know that the ratio of

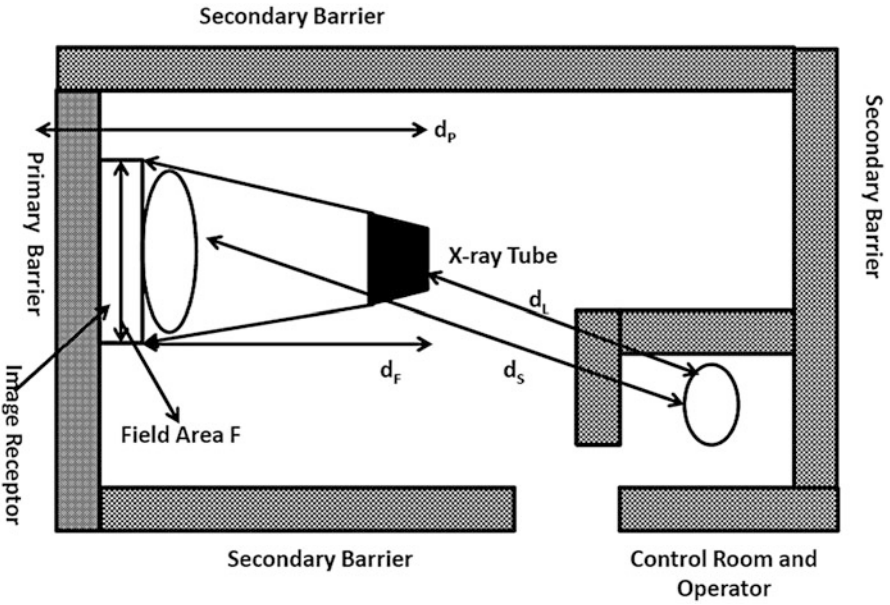

Fig. 13.17 Typical radiographic room

the measured KERMA at a detector and some known distance will be less than that with a barrier between the detector and the source. This is mathematically described in Eq. 13.30.

$$B(x) = \frac{K(x)}{K(0)} \tag{13.30}$$

These can be measured and fit to a solution called the Archer equation that uses three fit parameters. Solving this equation for thickness x, we get:

$$x = \frac{1}{\alpha\gamma} \ln\left[\frac{B^{-\gamma} + \frac{\beta}{\alpha}}{1 + \frac{\beta}{\alpha}}\right] \tag{13.31}$$

The specific fit values of a, b, and g are specific to the material being used as the barrier and cannot be listed here. Instead the report uses the transmission factor as parameter for evaluation, and tables in NCRP 147 give the thickness of the material needed to achieve the design goal. Equation 13.32 shows the calculation for the primary barrier:

$$B_{\text{primary}}\left(x_{\text{barrier}} + x_{\text{preshielding}}\right) = \frac{P}{T}\frac{d_P^2}{K_P^1 UN} \tag{13.32}$$

where

- B_{primary} – primary barrier transmission
- x_{barrier} – primary barrier thickness
- $x_{\text{preshielding}}$ – any attenuating thickness prior to the primary barrier
- P – shielding design goal
- T – occupancy factor
- D_{p} – distance to primary barrier
- $K^{1}{}_{\text{p}}$ – primary unshielded air kerma at 1 m per patient
- U – use factor
- N – number of patients

Secondary barriers are calculated using Eq. 13.33:

$$B_{\text{secondary}}(x_{\text{barrier}}) = \frac{P}{T}\frac{d^2_{\text{secondary}}}{K^1_{\text{sec}} N} \tag{13.33}$$

where

- B_{primary} – primary barrier transmission
- x_{barrier} – primary barrier thickness
- P – shielding design goal
- T – occupancy factor
- $K^{1}{}_{\text{sec}}$ – secondary unshielded air kerma at 1 m per patient
- N – number of patients
- $d_{\text{secondary}}$ – distance to secondary barrier

Values for several of these parameters require use of tables in NCRP 147. Common materials used for these barriers are lead, concrete, gypsum wall board, glass plated, steel, and wood. Of these lead is most commonly associated with diagnostic x-ray imaging.

13.6.1.2 NCRP 151 Methods

NCRP report 151 is focused on high-energy radiation beams although it shares many similarities to NCRP 147 in aspects discussed earlier. Once again the goal is to achieve sufficient shielding to reduce the exposure outside the room to the design goals which are the same as NCRP 147. Due to the nature of the higher energies (MeV vs. keV), several additional assumptions are made. These include, 30% attenuation of the primary beam by the patient, assumption of perpendicular distances to the primary barrier, leakage radiation assumed to be at maximum value, and conservative occupancy factors.

Calculation of the primary and secondary barriers is well defined based on the geometry of the radiation vault. In Fig. 13.18, the basic geometry is shown. Here the source to primary barrier is perpendicular to one another. The patient is in the beam path with secondary barriers being any wall that is not directly in the beam path. This means that any wall where the machine gantry rotates may be a primary

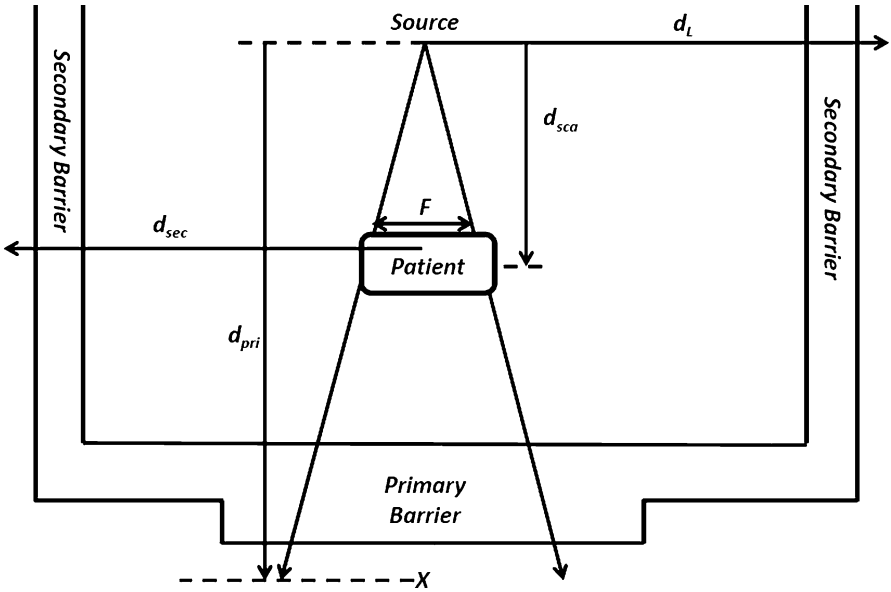

Fig. 13.18 NCRP 151 barrier thickness geometry

barrier. This includes the ceiling. Similar to diagnostic beams the patient is a source of scatter as is the leakage from the machine source housing. Unlike in NCRP 147 the leakage can be a large component of the secondary barrier transmission. This is a result of the fact that linear accelerators are high energy (4 MV–18 MV nominally). Note that in Fig. 13.18, the position x is the same as the reference position in NCRP 147 being 0.3 m from the wall as well as the same height, etc. It should be noted that linear accelerators may be run in photon and electron mode. Generally only the photon component is used in shielding calculations but as energy increases beyond 10 MV photon, neutrons may be produced. Consequently, addition of neutron shielding materials will need to be included. This usually involves the addition of borated polyethylene to the shield if concrete is not used (Fig. 13.18).

In Eq. 13.34 the calculation for the primary barrier is shown:

$$B_{\text{pri}} = \frac{P d_{\text{pri}}^2}{WUT} \tag{13.34}$$

where

- B_{pri} – transmission factor for primary barrier
- P – shielding design goal
- T – occupancy factor
- d_{pri} – distance to primary barrier
- U – use factor is the fraction of the workload directed to the primary barrier

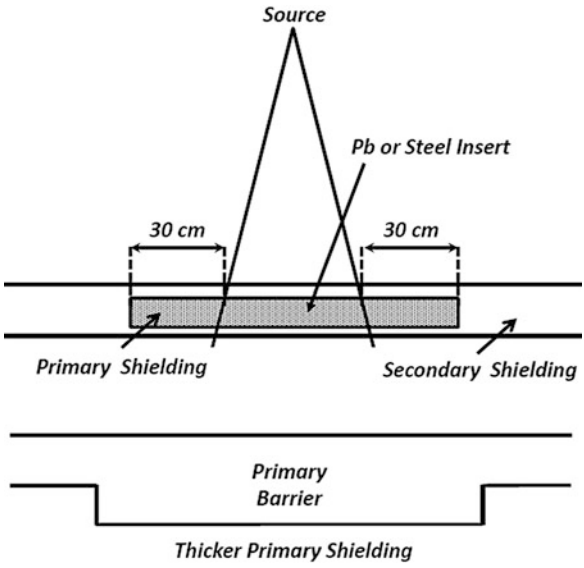

Fig. 13.19 Primary barrier design types

- W – workload or photon absorbed dose at 1 m from the target per week (Gy/wk)

To obtain the thickness from the transmission, one must use the data in the appendices of the NRCP 151 to obtain tenth value layers (TVL). A TVL is the thickness required to reduce the dose to one tenth its unshielded value. Then using this transmission factor the correct number of TVL is obtained by $n=-\log(B_{pri})$. Using n the total thickness fo the barrier is $t_{barrier}=TVL_1+(n-1)TVL_2$.

The primary barrier can be designed in several different ways. First the primary barrier may simply be a thickened wall that is 30 cm wider on each side of the maximum width of the treatment beam at the barrier wall. This is shown in Fig. 13.19 at the bottom of the figure. An alternate method may be to include a high-Z material inside of the primary barrier wall to further reduce the intensity of the beam as seen in the top of the same figure.

For secondary barriers two components are needed: the scatter from the patient and the leakage. Calculation of the secondary barrier is done using Eq. 13.35 and 13.36:

$$B_{sca} = \frac{P}{dWT} d_{sca}^2 d_{sec}^2 \frac{400}{F} \tag{13.35}$$

and

$$B_L = \frac{P d_L^2}{10^{-3} WT} \tag{13.36}$$

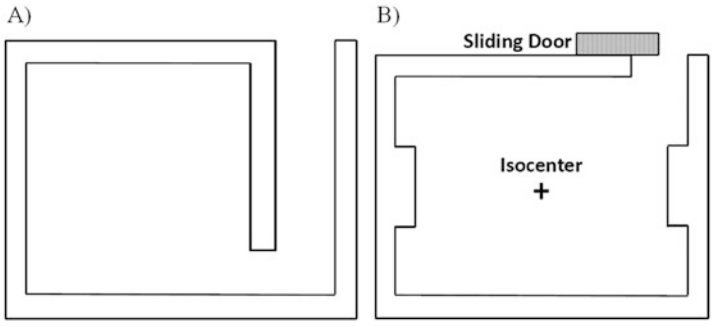

Fig. 13.20 (**a**) A maze design, (**b**) a maze less vault design

where

- d_{sca} – is the distance from the x-ray target to the patient
- d_{sec} – distance to the secondary barrier point
- a – scatter fraction: fraction of the beam that scatters to the secondary barrier
- F – size of field at midpoint of patient at isocenter (1 m)
- d_L – distance from source to secondary barrier

Determination of the thickness from the transmission values also requires review of the appendices in the report.

Additional computation is needed in the design of the vault. Two primary vault designs exist: maze and maze less. Each has their positive and negative aspects. Figure 13.20 shows these two designs. The maze design relies upon increasing the path through the vault that radiation may travel. It has the benefit of minimizing the amount of radiation shielding at the door. To do this does require more area for the vault to be built which can limit its application in some facilities. The mazeless design can be more compact and is appropriate in space limited situations. The major drawback is the size of the door needed to shield the room. These doors are very heavy requiring strong motors to move the system. Failure of these doors may increase risk to patients in the room. A hand crank mechanical device to open the door is always included in the design but does take time to open.

Construction of the vault should account for several factors including facility needs, future needs, location, and size of treatment room needed for the machine size. Thought should also go into workflow and storage needs. Plans for interlocks and the control console should also be well thought out prior to the project.

Common construction materials used in the linear accelerator shield projects include concrete (of varying densities), steel, rebar, and lead for photon components. Wood and earth are also often used although wood provides very little shielding. Earth is used for economic reasons, and it can be a logistic boon. For example, if the facility were built into the side of a hill and the vault location were adjacent to the hill, one of the barriers could use the thickness of the hill as shielding, thus saving costs of other shielding materials. Shielding materials for

neutron components include polyethylene and paraffin. Other consideration for construction of the vaults is unfortunately beyond the scope of this chapter. Review of the report in full is encouraged for complete details.

Additional Reading

Attix FH (2004) Introduction to radiological physics and radiation dosimetry. Wiley-VCH Verlag GmbH & Co. KGaA, Weinheim, Germany

Cember H (2008) Introduction to health physics, 4th edn. Thomas Johnson Publisher: McGraw-Hill Medical. ISBN-13: 978–0071423083

Martin JE (2013) Physics for radiation protection, 3rd edn. Wiley-VCH. ISBN-13: 978–3527411764

Nahum A (2007) Principles and basic concepts in radiation dosimetry. In: Mayles P, Nahum A, Rosenwald JC (eds) Handbook of radiotherapy physics: theory and practice. CRC Press, pp. 89–114

Orabi M (2017) Radon release and its simulated effect on radiation doses. Health Phys 112 (3):294–299

Podgorsak EB (2005) External photon beams: physical aspects. In: Podgorsak EB (ed) Radiation oncology physics: a handbook for teachers and students. International Atomic Energy Agency (IAEA), Vienna, pp 161–217

Stabin MG (2007) Radiation protection and dosimetry: an introduction to health physics. Springer Science & Business Media, pp. 67–74

United States Nuclear Regulatory Commission: NUREG-1556 Vol-9 Rev 2: Consolidated Guidance About Materials Licenses Program-Specific Guidance About Medical Use Licenses, Final Report, Published: January 2008; Prepared by D.B. Howe, M. Beardsley, S. Bakhsh, Office of Federal and State Materials and Environmental Management Programs